Vibrational and collisional energy effects in the reaction of ammonia ions with methylamine

Jonathan E. Flad, Michael A. Everest,[a] John C. Poutsma,[b] and Richard N. Zare[c]
Department of Chemistry, Stanford University, Stanford, California 94305

(Received 16 November 2000; accepted 16 April 2001)

We have investigated the reactions of vibrationally state-selected ammonia ions with d_3-methylamine over the center-of-mass collisional energy range of 0.5 to 10.0 eV and for ammonia ion vibrational states ranging from $\nu_2=1-9$. Under these conditions, five major products appear: NH_4^+, NH_3D^+, $CD_2NH_2^+$, $CD_3NH_2^+$, and $CD_3NH_3^+$. The cross section for each product is a decreasing function of collision energy and also a decreasing function of energy in the ν_2 mode of the ammonia ion, except for $CD_2NH_2^+$ that shows about a twofold enhancement with increasing internal energy, most notably at low-collision energies. Examination of the velocity scattering profiles shows that the mechanism for formation of each major product does not involve complex formation in this energy range. Branching ratios for each product are measured, and a comparison is presented for $CD_2NH_2^+$ and $CD_3NH_2^+$ arising from reactions with ammonia ions prepared in two nearly isoenergetic states. One state has no quanta in the symmetric stretch and five quanta in the umbrella bending mode (1^02^5) and the other has one quantum in the symmetric stretch and two quanta in the umbrella bending mode (1^12^2). Comparison indicates that this reaction is vibrationally mode selective, although the extent of mode selectivity is small. © *2001 American Institute of Physics.* [DOI: 10.1063/1.1377605]

I. INTRODUCTION

Ion–molecule reactions play an important role in many chemical environments including plasmas, upper atmospheric chemistry, interstellar space, and the environment of low-Earth orbiting spacecraft.[1] To understand better the effects of different types of energy and the partitioning of that energy on reactivity, we have studied the NH_3^+–CD_3NH_2 system. In particular, we examine how collision energy, ion internal energy, and ion vibrational mode influence the reaction efficiency, product branching, and product scattering. Because single-collision conditions are maintained, the measurement of product recoil velocity distributions helps us gain insight into the elementary reaction mechanism producing each product. Also, by measuring cross sections as a function of collision energy and internal energy, we observe the competition between these two types of energy in governing the outcome of a chemical reaction. The present study allows us to determine whether it is the total energy of the system or the partitioning of that energy that controls the reaction outcome.

The NH_3^+–CD_3NH_2 system is interesting for several reasons. First, previous to this study, this laboratory has examined reactions of ammonia ions with small hydrides, such as D_2, D_2O, CD_4, and ND_3, exclusively.[2–5] Methylamine, though still small by chemical standards, offers a reaction where many more product channels are energetically open (27 internal degrees of freedom). Second, in those previous studies we have hypothesized that mode selectivity in ion–molecule reactions involving the ammonia ion is driven by the Franck–Condon overlap between the vibrationally excited ammonia ion and the neutral ammonia resulting from charge transfer.[6] The NH_3^+–CD_3NH_2 system is an excellent test of this hypothesis because this system has an exothermic change transfer channel. Finally, the ammonia ion is one of the few ions that can be prepared with a wide variety of specific internal states owing to the nature of the multiphoton ionization scheme utilized.[7]

State-selected ion–molecule reactions involving methylamine as the neutral target have been studied before using phenol as the state-selected ion.[8] In that reaction, proton transfer was the only product seen at the collision energies studied, 0.1–2 eV. The cross section for formation of this product was found to be a decreasing function of collision energy for the three different ion preparations studied. Excitation into two different normal modes of the phenol ion also inhibits reactivity over the collision energy range. It was also found that the product ion velocity distributions show nearly perfect forward–backward symmetry at low-collision energies, which indicates a mechanism mediated by complex formation.

Adams, Smith, and Paulson[9] reacted ammonia ions with methylamine at thermal collisional energies in a selected ion flow tube (SIFT). Under their experimental conditions, they observed three major products corresponding to charge transfer (50%), proton transfer (35%), and hydrogen abstraction (15%). They found the binary rate constant for this reaction to be 1.8×10^{-9} under energetically thermal conditions,

[a]Present address: Department of Chemistry, Trinity University, San Antonio, TX 78212.
[b]Present address: Department of Chemistry, College of William and Mary, Williamsburg, VA 23187.
[c]Electronic mail: zare@stanford.edu

comparable with the theoretical [average dipole orientation (ADO)] value of 2.06×10^{-9}.

The reaction of ammonia ions with d_3-methylamine under hyperthermal energetic conditions presented here also produces charge transfer, proton transfer, and hydrogen abstraction, along with several other products. Shown below are the energetics for some possible products of this reaction

$$\mathrm{NH_3^+ + CD_3NH_2 \rightarrow} \begin{cases} \mathrm{NH_4^+ + CD_3NH} & \approx -0.9\ \mathrm{eV} \\ \mathrm{NH_2D^+ + CD_2NH_2 + H} & \approx +4.2\ \mathrm{eV} \\ \mathrm{NH_3D^+ + CD_2NH_2} & \approx -1.2\ \mathrm{eV} \\ \mathrm{NH_3 + CD_2NH_2^+ + D} & \approx +0.1\ \mathrm{eV} \\ \mathrm{NH_2 + CD_2NH_2^+ + HD} & \approx +0.3\ \mathrm{eV} \\ \mathrm{NH_3 + CD_3NH_2^+} & \approx -1.1\ \mathrm{eV} \\ \mathrm{NH_2 + CD_3NH_3^+} & \approx -1.0\ \mathrm{eV} \end{cases} \quad (1)$$

The energies reported are ΔH_{rxn} at 298 K.[10] Note that two different reactions produce products with $m/z=18$ and 32.

II. EXPERIMENT

The experimental method used in this study has been described in detail elsewhere.[11] Briefly, ammonia cations are produced in specific vibrational states using (2+1) resonance-enhanced multiphoton ionization (REMPI) by crossing a pulsed molecular beam of ammonia (5% in He) with the frequency-doubled output of a NG:YAG pumped dye laser. Two normal modes of the ammonia cation can be accessed using this arrangement. The ν_1 symmetric stretching (''breathing'') mode can be prepared with either zero or one quanta, whereas the ν_2 symmetric bending (''umbrella'') mode can be excited with zero to ten quanta of energy.[12,13] A particular vibrational state is described as 1^m2^n where m is the number of quanta in the ν_1 mode and n is the number of quanta in the ν_2 mode. The ions are extracted orthogonally from the ionization region by a direct current (dc) turning quadrupole and injected into a quadrupole mass filter that selects only those reactant ions with the correct mass-to-charge ratio ($m/z=17$). The reactant ions are then focused into an octopole ion guide[14] that is concentric with a collision cell containing the neutral target gas (methylamine-d_3, Cambridge Isotope Laboratory, 98% D). The d_3-methylamine is introduced through a leak valve to obtain a pressure in the collision cell of ~30 μTorr. The octopole ion guide ensures that all ions with some forward component of velocity in the lab frame are collected and focused into the second quadrupole for mass analysis. Ion detection is carried out using fast microchannel plates. Using a multichannel scaler and a current transient recorder, time-of-flight profiles for both product and reactant ions are measured sequentially.

The collision energy between the ammonia ions and neutral methylamine is controlled by varying the dc pole offset of the octopole ion guide relative to the field-free ionization region, which is kept constant at ground. The laboratory-frame collision energy, E_{LAB}, set by the dc pole offset on the octopole rods can be converted into the center-of-mass frame collision energy, E_{CM}, according to $E_{\mathrm{CM}}=E_{\mathrm{LAB}}[m/(m+M)]$, where m is the mass of the neutral molecule and M is the mass of the ion. Thus, a voltage range of -0.75 to -15.00 V on the octopole rods corresponds to a center-of-mass collision energy range of 0.50–10.0 eV.

We report relative integral cross sections calculated by normalizing the counted signal for a particular product ion to the integrated current of the unreacted ammonia ions. The term ''relative'' refers to the fact that we are unable to measure absolute cross sections because we know neither the exact pressure in the collision cell nor the effective path length. Because the pressure in the collision cell was kept nearly constant for all of the experiments reported here, all of the cross sections presented in this work can be compared with each other. We also report product branching ratios, calculated by dividing the counted intensity of a particular product ion by the counted intensity of all product ions under the same experimental conditions. Although branching ratios contain less information than relative cross sections, they have the advantage of dividing out any experimental error that has an equal multiplicative effect on all products.

Owing to the timing of the experiment, where a short laser pulse ($\approx$10 ns) determines the start time and a time-sensitive detector ($\tau<5$ ns) counts the ions, the time-of-flight of the product ions can be measured. If the instrument function is well known, then the time-of-flight profiles can be converted into the velocity domain yielding information about the reactive scattering of the ion products. The instrument function is estimated by simulating the guided-ion beam to determine the correlation between ion flight time and ion velocity in the octopole. The velocity profiles reported here are a histogram vs the projection of the product velocity onto the instrument axis. The instrument axis is coincident to the initial velocity of the ammonia ions and, therefore, to the velocity of the center-of-mass because the average speed of the CD_3NH_2 is small compared to the speed of the ammonia ion. Therefore, although a complete differential cross section cannot be measured using this instrument, the velocity histogram can accurately yield information on the degree of forward or backward scattering.

III. RESULTS AND DISCUSSION

A. Low-mass products

1. Collisional energy dependence

The minor products with mass-to-charge ratio of 18 and 19 have been identified as hydrogen abstraction, NH_4^+, and deuterium abstraction, NH_3D^+, respectively. There is also evidence in the scattering data that a small amount of formal isotope exchange, NH_2D^+, also takes place under the experimental conditions studied. Figure 1 shows the collisional energy dependence of these low-mass channels for the reaction of $NH_3^+(1^02^5)+CD_3NH_2$. The data in this figure and all subsequent figures represent the mean of at least three data sets while the error bars represent one standard deviation for those data sets. The relative cross sections for both channels are decreasing functions of the center-of-mass collision energy. The cross section for hydrogen abstraction drops abruptly by just less than a factor of 3 in going from 0.5 to 2.0 eV, then levels off upon increasing the collision energy

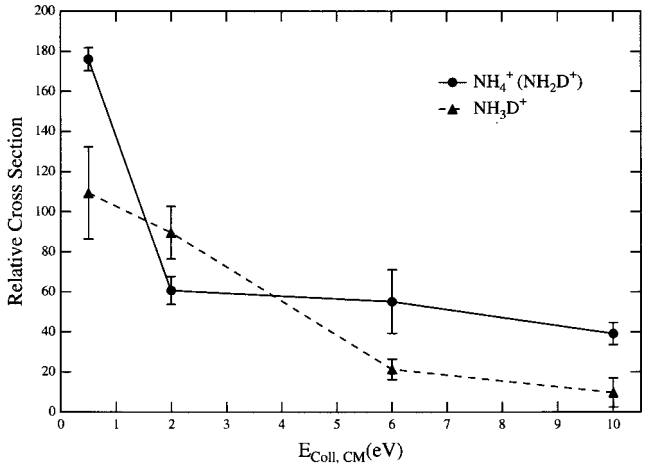

FIG. 1. Relative reaction cross sections (arbitrary units) for the reaction of NH_3^+ (1^02^5)+CD_3NH_2 as a function of center-of-mass collision energy to form NH_4^+ (NH_2D^+) and NH_3D^+. The error bars represent one standard deviation ($\pm s$).

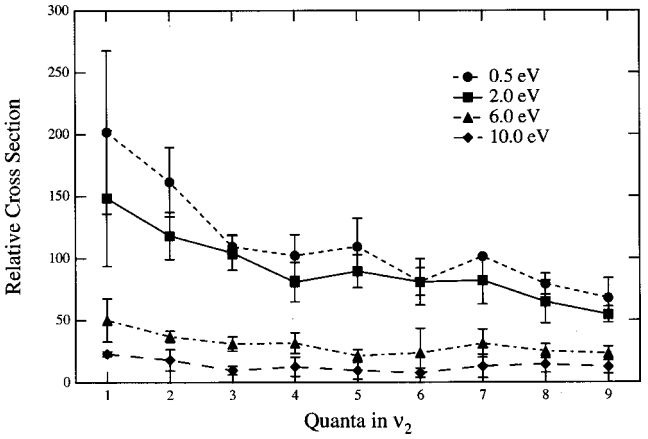

FIG. 3. Relative reaction cross sections (arbitrary units) for the formation of NH_3D^+ as a function of ammonia–ion vibrational state (quanta in ν_2) at the center-of-mass collision energies of 0.5, 2, 6, and 10 eV. The error bars represent one standard deviation ($\pm s$).

from 2.0 to 10 eV. The cross section of deuterium abstraction, on the other hand, decreases smoothly by about a factor of 10 upon increasing the collision energy from 0.5 to 10 eV.

The behavior of these channels with respect to collision energy is very similar to the deuterium abstraction channel observed in the reaction of ammonia ion with methane ($NH_3^+ + CD_4 \rightarrow NH_3D^+ + CD_3$).[4] This type of behavior, where the cross section is a decreasing function of collision energy, is typical for ion–molecule reactions with no threshold energy.

2. Vibrational energy dependence

Figures 2 and 3 show the dependence of the relative cross sections for the formation of NH_4^+ and NH_3D^+ on the number of quanta excited in the ν_2 mode of the ammonia ion. All collision energies studied are shown in the figures. The amount of internal energy ranges from 0.12 to 1.08 eV in going from $\nu_2 = 1-9$. This amount is about one-tenth of the collision energy range. Both abstraction channels are inhibited with increasing energy in the ν_2 mode of the ammonia ion. These trends are most notable at the lower collision energies where the cross section for hydrogen abstraction decreases by about a factor of 2 at 0.5 and 2.0 eV. The cross section for deuterium abstraction decreases by just less than three times for the two lowest collision energies. At higher collision energies (6.0 and 10 eV) the cross sections for H- and D-abstraction are essentially unaffected by vibrational excitation of the umbrella bending mode of the NH_3^+.

Upon inspection of the figure illustrating the collisional energy dependence of these two channels (Fig. 1), it is clear that for both abstraction channels, the trend in vibrational energy is very similar to the trend seen vs collision energy when viewed over the same energy range (about 1 eV). Therefore, it is the sum of vibrational and collision energy that governs the cross sections of these two products. The partitioning of the energy between vibration and collision seems to have little to no effect on the outcome of the abstraction reactions for this system.

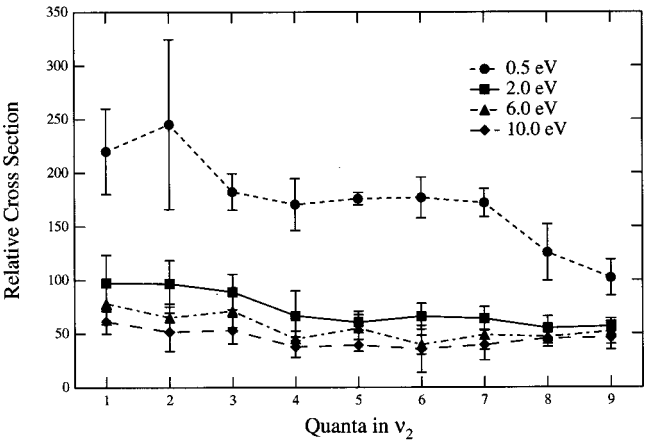

FIG. 2. Relative reaction cross sections (arbitrary units) for the formation of NH_4^+ (NH_2D^+) as a function of ammonia–ion vibrational state (quanta in ν_2) at the center-of-mass collision energies of 0.5, 2, 6, and 10 eV. The error bars represent one standard deviation ($\pm s$).

3. Product scattering

Figures 4 and 5 show the velocity profiles of the H- and D-abstraction products in the laboratory frame at four different collision energies. The velocity of the center-of-mass as well as the prediction of the spectator-stripping model is indicated by the vertical lines. The spectator-stripping model assumes that no momentum is transferred during the reactive encounter. In the case of abstraction, the velocity of the neutral CD_3NH (CD_2NH_2) fragment is equal to the initial velocity of the CD_3NH_2 reagent. This limit is calculated in the case of H-abstraction according to

$$w_{NH_4^+} = \frac{m_{CD_3NH}}{m_{NH_4^+}} \sqrt{\frac{2E_{CM}m_{NH_4^+}}{Mm_{CD_3NH_2}}},$$

where m_i is the mass of species i in kilograms, w_i is the center-of-mass frame velocity of species i in meters per sec-

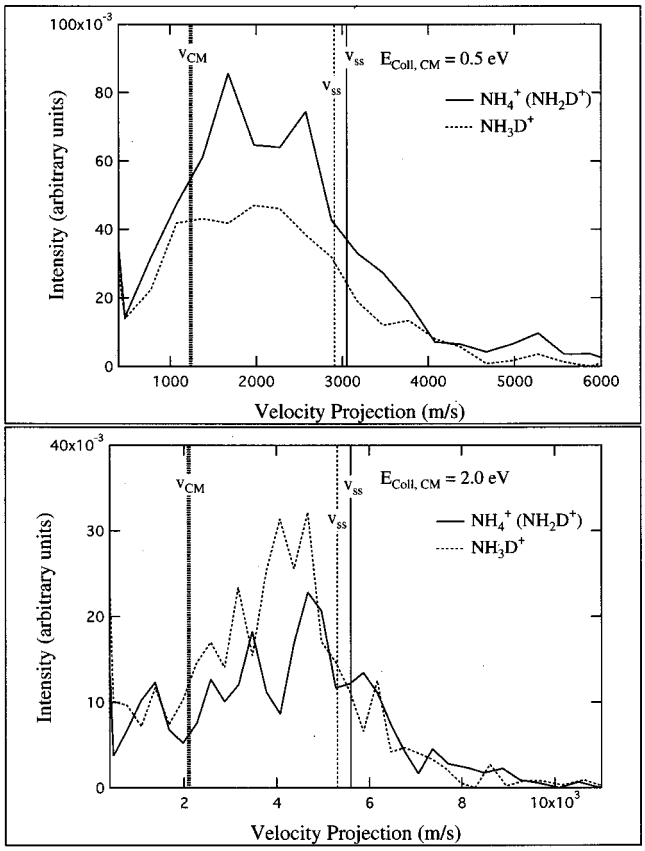

FIG. 4. Laboratory-frame velocity histograms for NH_4^+ (NH_2D^+) and NH_3D^+ at center-of-mass collision energies of 0.5 and 2.0 eV. The velocity of the center-of-mass and the predictions of the spectator-stripping model are shown.

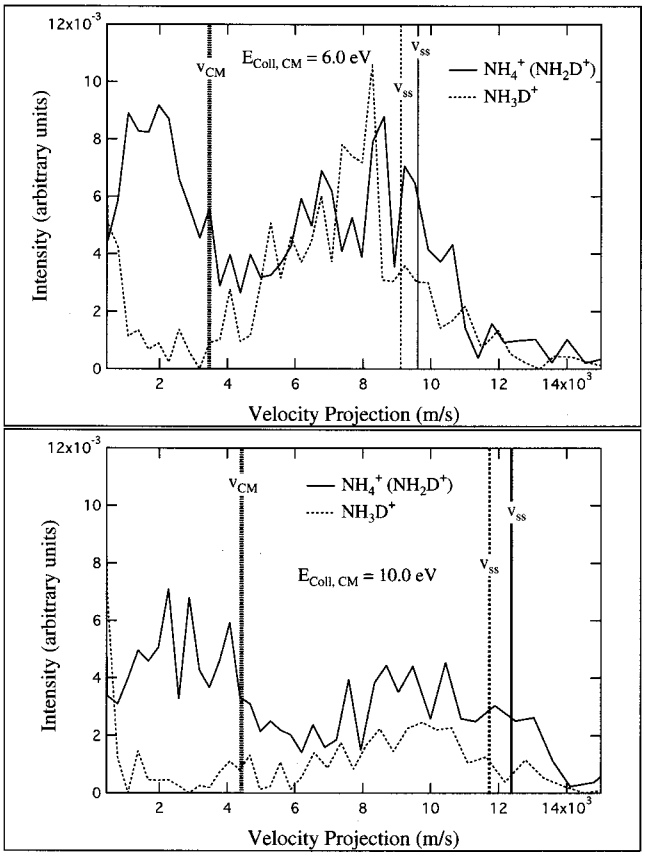

FIG. 5. Laboratory-frame velocity histograms for NH_4^+ (NH_2D^+) and NH_3D^+ at center-of-mass collision energies of 6.0 and 10 eV. The velocity of the center-of-mass and the predictions of the spectator-stripping model are shown.

ond, and M is the total mass of the system in kilograms. For both H- and D-abstraction, the velocity profiles are seen to scatter predominately in the forward direction where they approach the spectator-stripping limit.

This type of scattering is typical for ion–molecule reactions because of the large impact parameters characteristic of the strong charge-induced dipole forces that tend to dominate these systems. This type of near spectator-stripping scattering is similar to scattering observed for $NH_3D^+(NH_3^+ + CD_4 \rightarrow NH_3D^+ + CD_3)$[4] and $D_2OH^+(NH_3^+ + D_2O \rightarrow D_2OH^+ + OD)$.[3]

Interestingly, the velocity profile of the $m/z = 18$ channel indicates that two different products or mechanisms may compete above 4 eV. Because product detection is achieved using a quadrupole mass filter and microchannel plates, differing scattering dynamics is a unique way to differentiate products having the same mass-to-charge ratio. Figure 5 shows that at 6 eV, a substantial amount of product begins to scatter slightly in the backward direction, which indicates, perhaps, a different mechanism for producing a product with $m/z = 18$. A reaction that accounts for this observation is formal isotope exchange, $NH_2D^+ + CD_2NH_2 + H$ ($\Delta H_{rxn} \approx 4.2$ eV). A possible mechanism for formation of NH_2D^+ is a two-step process: collision-induced dissociation of the ammonia ion resulting in the formation of a short-lived $[NH_2CD_3NH_2]^+$ complex that decays to products. This laboratory has investigated three other systems that result in the same type of isotope exchange product with a threshold for formation of about 4 eV, namely reactions of ammonia ions with D_2, D_2O, and CD_4. In the reaction with D_2, the precise mechanism for the formation of NH_2D^+ could not be determined owing to the kinematics of the system (the center-of-mass of the system nearly coincides with the ammonia ion throughout the reactive encounter). However, this type of isotope exchange mechanism or a direct stripping mechanism followed by decay of the NH_3D^+ product is thought to describe the mechanism in that case. In the $NH_3^+ - CD_4$ system, the mechanism thought to describe the CD_3^+ product is also collision-induced dissociation of the ammonia ion or methane molecule, resulting in a short-lived complex that then decays to products. Like the NH_2D^+ product in the present system, the CD_3^+ product was also seen to be slightly backward scattered, indicating that the lifetime of the complex is less than a typical rotational period.

Another mechanism, suggested by the referee, that explains the appearance of NH_2D^+ is unimolecular decomposition of NH_3D^+ formed via small impact parameter collisions. This mechanism accounts for the slightly backward-scattered velocity distribution of the product whereby D-abstraction, from small impact parameter collisions, results in backward-scattered NH_3D^+ with enough internal energy to rupture a N–H bond. Large impact parameter collisions lead to stable NH_3D^+ that is forward scattered. At

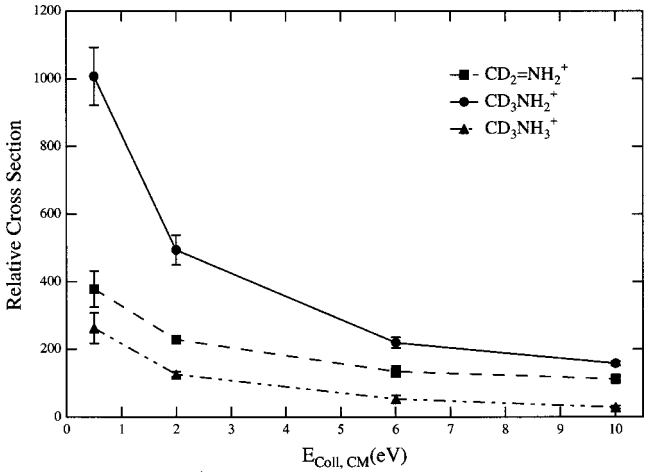

FIG. 6. Relative reaction cross sections (arbitrary units) for the reaction of $NH_3^+(1^02^5)+CD_3NH_2$ as a function of center-of-mass collision energy to form $CD_2{=}NH_2^+$, $CD_3NH_2^+$, and $CD_3NH_3^+$. The error bars represent one standard deviation ($\pm s$).

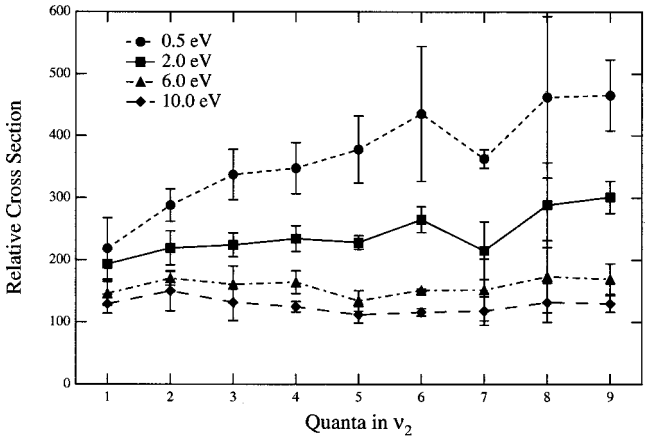

FIG. 7. Relative reaction cross sections (arbitrary units) for the formation of $CD_2{=}NH_2^+$ as a function of ammonia–ion vibrational state (quanta in ν_2) at the center-of-mass collision energies of 0.5, 2, 6, and 10 eV. The error bars represent one standard deviation ($\pm s$).

low-collision energies (Fig. 4) there is both forward and backward-scattered products for $m/z=18$ and $m/z=19$ (NH_4^+ and NH_3D^+) formed by direct hydrogen or deuterium abstraction, respectively. These distributions are nearly identical, suggesting a common abstraction mechanism. As the collision energy is increased (Fig. 5), the amount of backward-scattered $m/z=18$ product increases while the amount of backward-scattered $m/z=19$ product decreases. Small impact parameter collisions are effective in driving kinetic to vibrational energy transfer, whereas large impact collisions are effective in driving kinetic to rotational energy transfer. Consequently, as the collision energy is increased, NH_3D^+ formed from small impact parameter collisions become progressively more vibrationally excited until, at 6 eV, there is enough internal energy available to decompose NH_3D^+ by H- or D-atom loss. Figure 5 shows that as the backward-scattered component of the $m/z=18$ velocity distribution increases, an analogous decrease in the backward-scattered component of the $m/z=19$ distribution occurs, as would be expected for NH_3D^+ decomposition to NH_2D^+. We are presently unable to distinguish between these two possible mechanisms and perhaps both mechanisms are competing.

B. High-mass products

1. Collisional energy dependence

Figure 6 shows the collisional energy dependence of the high-mass channels in the reaction of $NH_3^+(1^02^5)+CD_3NH_2$. The most abundant product at all collision energies is exothermic charge transfer, $CD_3NH_2^+$. Products corresponding to dissociative charge transfer ($CD_2{=}NH_2^+$) and proton transfer ($CD_3NH_3^+$) have also been identified, in part, by results from isotopic substitution experiments involving ND_3^+ as the reagent ion and CD_3ND_2 as the neutral target. Like the abstraction products discussed above, the relative cross sections for formation of all three products are decreasing functions of collision energy at the hyperthermal energies studied. Increasing the collision energy from 0.5 to 10 eV causes just over a threefold decline in the cross section for $CD_2{=}NH_2^+$, a sixfold decline in the cross section for $CD_3NH_2^+$, and an ninefold decline in the cross section for $CD_3NH_3^+$. The drop in these cross sections is comparable to the decline seen above in the abstraction products. Like the abstraction products, we attribute the drop in each individual cross section to result from the overall decline of the total collision cross section with increasing collision energy, in accordance with the Langevin model.[15]

2. Vibrational energy dependence

The vibrational energy dependence on the relative cross sections for $CD_2{=}NH_2^+$ and $CD_3NH_2^+$ are shown in Figs. 7 and 8. Each point represents the mean of at least three data sets and the error bars represent one standard deviation for those data sets. It is interesting to note that $CD_2{=}NH_2^+$ is the only product that shows an enhancement in its cross section upon increasing energy in the ν_2 mode of the ammonia ion. This trend is the greatest at the lowest two collision energies studied. The cross section increases by a factor of 2 and 1.6

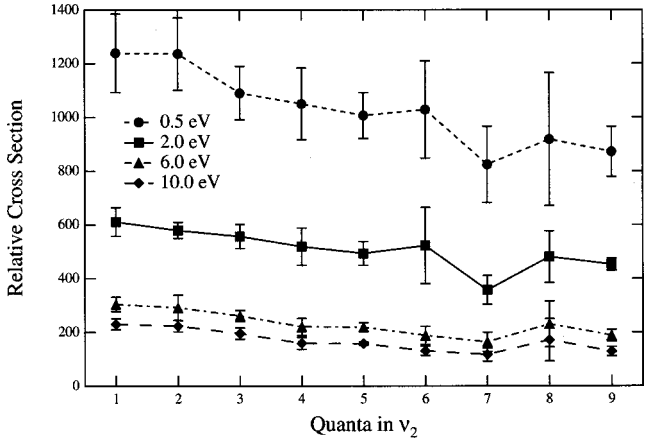

FIG. 8. Relative reaction cross sections (arbitrary units) for the formation of $CD_3NH_2^+$ as a function of ammonia–ion vibrational state (quanta in ν_2) at the center-of-mass collision energies of 0.5, 2, 6, and 10 eV. The error bars represent one standard deviation ($\pm s$).

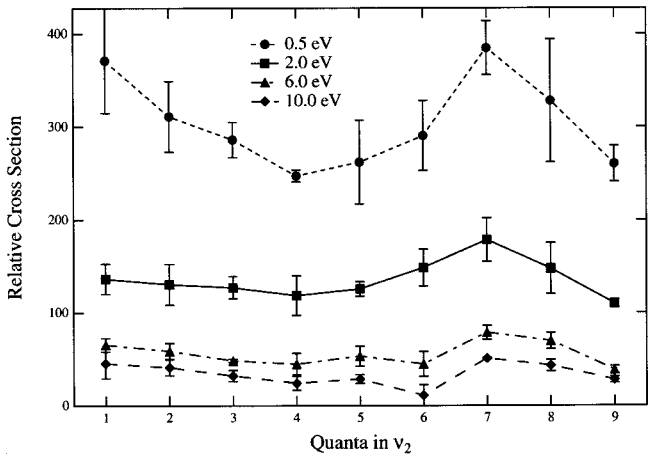

FIG. 9. Relative reaction cross sections (arbitrary units) for the formation of $CD_3NH_3^+$ as a function of ammonia–ion vibrational state (quanta in ν_2) at the center-of-mass collision energies of 0.5, 2, 6, and 10 eV. The error bars represent one standard deviation ($\pm s$).

at 0.5 and 2.0 eV, respectively. Above these energies, the amount of vibrational energy shows no influence in the formation of the dissociative charge transfer product. Figure 8 shows that the cross section for the charge-transfer product decreases slightly at all collision energies studied. The cross section for proton transfer (Fig. 9) decreases by less than a factor of 2 at all collision energies after increasing and peaking at $\nu_2=7$. More investigation needs to be performed in order to explain the nonmonotonic behavior of the proton channel with ν_2 excitation. We believe, however, that this behavior is quite real because there appears to be a corresponding nonmonotonic decline in the cross sections for charge transfer and dissociative charge transfer at $\nu_2=7$, especially at low-collision energies.

As in the case of the abstraction products, it is the total energy of the system, instead of the specific partitioning of that energy that governs the production of $CD_3NH_2^+$. The cross section for charge-transfer drops to the same extent with respect to internal energy as it does over the same collision energy range (about 1 eV). On the other hand, dissociative charge transfer is enhanced by vibrational energy whereas it decreases with increasing collision energy. One possible explanation for this behavior is that changing Franck–Condon factors with increasing ν_2 excitation may increase partitioning of the available energy to internal energy of the charge-transfer product, thereby enhancing dissociation.

3. Product scattering

Figures 10 and 11 show the velocity profiles for the charge transfer, dissociative charge transfer, and proton transfer products in the laboratory frame at a collision energies of 0.5 and 2.0 eV and 6.0 and 10 eV, respectively. The vertical line shows the center-of-mass velocity. All three products are backward scattered at all four collision energies studied, indicating mechanisms not mediated by complex formation. Because the velocity profiles of the charge transfer product are backward scattered at each collision energy studied, we conclude that the mechanism for charge transfer

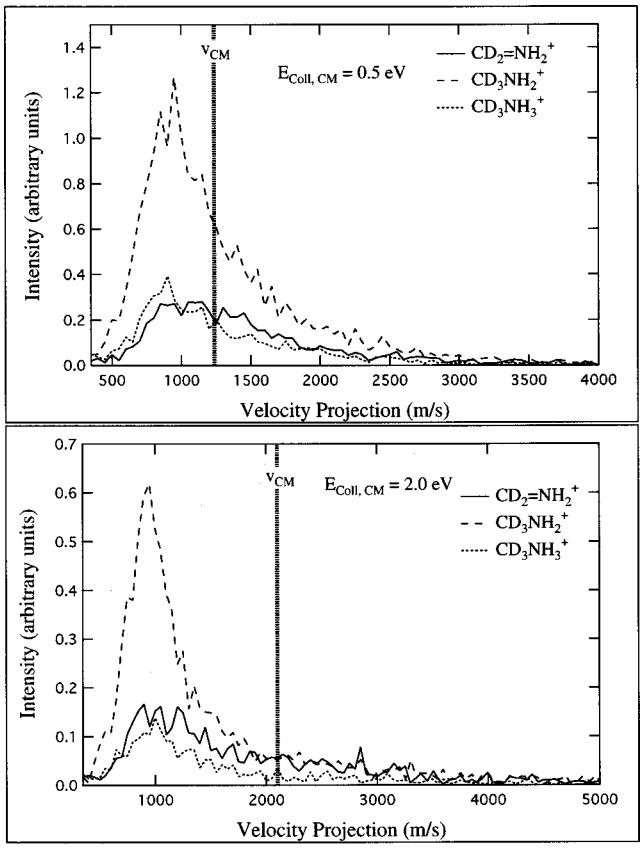

FIG. 10. Laboratory-frame velocity histograms for $CD_2{=}NH_2^+$, $CD_3NH_2^+$, and $CD_3NH_3^+$ for center-of-mass collision energies of 0.5 and 2.0 eV. The velocity of the center-of-mass is also shown.

in this system is dominated by long-range electron transfer. Long-range charge transfer is not always the dominant mechanism for large reactant molecules. For example, charge transfer to phenol from ND_3^+ requires intimate collisions for which considerable momentum transfer to the phenol cation occurs.[16] This mechanism, intermediate between long-lived complex formation and long-range electron hopping, may also be important for charge transfer to methylamine at or below 0.5 eV via a hydrogen-bonded complex. The velocity profile for dissociative charge transfer lies almost exactly under the profile for charge transfer, providing evidence that the mechanism for formation of $CD_2{=}NH_2^+$ is a two-step process, electron transfer followed by a dissociation reaction that occurs on the charge-transfer surface. Nevertheless, because the velocity distributions of all three high-mass products are similar, we cannot rule out the possibility that another mechanism operates, whereby first proton transfer occurs followed by loss of molecular hydrogen (HD). Both mechanisms (dissociative charge transfer and dissociative proton transfer) may, in fact, be competing.

C. Mode selectivity

The degree of vibrational mode selectivity in ion–molecule reactions involving NH_3^+ can be determined by comparing the reactivity of ammonia ions prepared in nearly isoenergetic states with differing concerted motion of the ion's nuclei. In particular, Fig. 12 compares the reactivity of

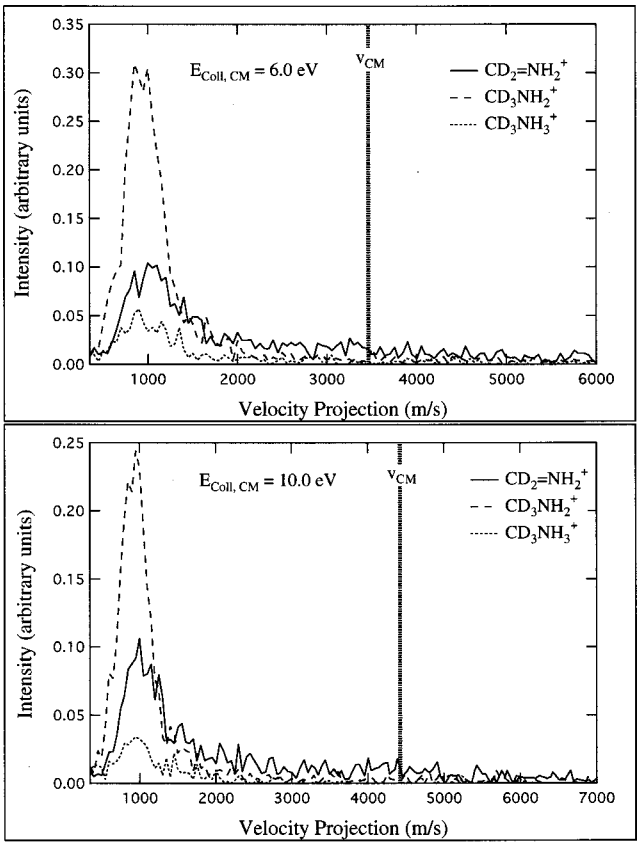

FIG. 11. Laboratory-frame velocity histograms for $CD_2{=}NH_2^+$, $CD_3NH_2^+$, and $CD_3NH_3^+$ for center-of-mass collision energies of 6.0 and 10 eV. The velocity of the center-of-mass is also shown.

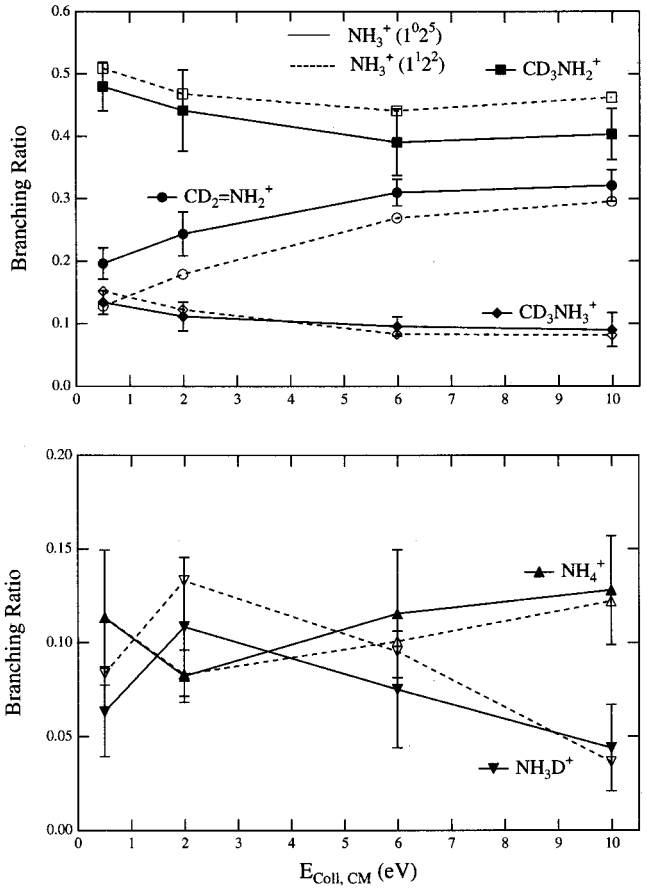

FIG. 12. Product branching ratios as a function of center-of-mass collision energy. Reactions of both NH_3^+ ($1^0 2^5$) (E_{int}=0.60 eV) and NH_3^+ ($1^1 2^2$) (E_{int}=0.63 eV) are shown. Error bars represent the pooled standard deviation for both sets of data multiplied by Student's *t* at a 95% confidence level (ts_{pooled}).

ammonia ions prepared with one quantum in the ν_1 all-symmetric stretching mode and two quanta in the ν_2 symmetric bending mode ($1^1 2^2$; E_{int}=0.63 eV) with ammonia ions prepared with five quanta in the ν_2 symmetric bending mode ($1^0 2^5$; E_{int}=0.60 eV). Product branching ratios for each product are displayed as a function of center-of-mass collision energy. Branching ratios are used to demonstrate mode selectivity because they have the advantage of canceling out any experimental error that has an equal multiplicative effect on all products. The amount of NH_3^+ formed in the combination state ($1^1 2^2$) is about one-third the amount produced in any of the pure bending states. The scheme we use to integrate the analog signal to calculate cross sections is nonlinear for small reactant peak heights. This treatment causes underestimation of reactant signal that, in turn, leads to cross sections that are systematically larger than their true value, making comparison of the $1^1 2^2$ and $1^0 2^5$ cross sections difficult. The error bars in the figure represent the pooled standard deviation for both sets of data multiplied by Student's *t* at a 95% confidence level (ts_{pooled}).[17] The degree of mode selectivity in this reaction can be deduced from the branching ratios by determining the extent of overlap between the error bars on the one set of data with the other data set. Comparison of the branching ratios for the charge transfer and dissociative charge transfer channels indicates that this reaction is vibrationally mode specific.

More dramatic instances of mode specificity are known, such as the reactions of H atoms[18–21] and Cl atoms[22] with vibrationally excited HOD molecules, where H or Cl selectively abstracts either the H or D atom from HOD depending on the vibrational excitation of the HOD reagent. Nevertheless, mode selectivity is clearly present in this reaction and has been observed before in reactions involving ammonia ions in this laboratory[6,23] and by Anderson *et al.*[24] In each ammonia ion/molecule reaction where mode selectivity is observed, the system has an open charge transfer channel. The charge transfer reaction in this system involves fast electron transfer. Evidence for this direct mechanism is supported by the fact that we do not observe forward-backward symmetry in the velocity distributions (Figs. 10 and 11). Furthermore, the electron transfer is fast compared to the time scale of nuclear motion. Because we observe differences in reactivity based on the particular preparation of the ammonia ion, we can conclude that the internal energy of the ammonia ion has not had time to relax or be randomized via intramolecular vibrational relaxation throughout the course of the experiment. It should be pointed out that this experiment takes hundreds of microseconds to perform whereas the time for state-selected ions to relax has been determined to be on the order of milliseconds.[25] Therefore, the observed difference in reactivity is a direct result of the concerted motion of the nuclei of the ammonia ion. This reaction, with 27 degrees

of internal freedom, represents one of the largest systems for which mode selectivity has been demonstrated.

Unlike the $NH_3^+ + ND_3$ system, it is not the charge-transfer channel that is enhanced by having more energy in the ν_2 mode of the ammonia ion. Rather, dissociative charge transfer is enhanced primarily at the expense of the charge transfer channel in going from ammonia ions prepared in $1^1 2^2$ to $1^0 2^5$. This conclusion is consistent with Fig. 7 that plainly shows that the dissociative charge transfer product is the only product of this reaction that is enhanced with increasing quanta in the ''umbrella'' bending mode of the ammonia ion. Moreover, this fact lends further evidence to our conclusion that the channel with $m/z=32$ is dissociative charge transfer because the only ion–molecule reactions involving ammonia ions that have been shown to be mode selective are those where charge transfer products have been observed. Similar behavior is seen in another reaction studied in this laboratory, $NH_3^+ + THF$.[6] As in the methylamine reaction, a dissociative charge-transfer product was seen to be enhanced with increased partitioning of the internal energy into the ν_2 mode of the ammonia ion.

It is no coincidence that reactions involving ammonia ions display mode selectivity only when there is an energetically open charge transfer channel ($NH_3^+ + ND_3$, C_4H_8O, and CD_3NH_2). In reactions involving the ammonia ion where the charge-transfer channel is energetically closed ($NH_3^+ + D_2$, D_2O, and CD_4) no mode selectivity is observed. We ascribe the mode selectivity seen in this reaction of NH_3^+ with d_3-methylamine, and in ammonia ion–molecule reactions in general, to result from increased Franck–Condon overlap between the ammonia molecule excited in the ν_2 vibrational mode and the nascent neutral ammonia molecule resulting from charge transfer. This explanation is the inverse of the same principle that explains the ability of ammonia ions to be prepared with varying degrees of excitation in the ν_2 vibrational mode. Thus, it appears that in systems with many degrees of freedom, the identity of the neutral reagent molecule is unimportant as long as it can donate an electron to the ammonia ion. Further work is required to determine how general this behavior is.

IV. CONCLUSIONS

The reaction of ammonia molecules with d_3-methylamine produces five primary products in the center-of-mass collision energy range of 0.5–10 eV. The most abundant product at all collision energies results from exothermic electron transfer ($CD_3NH_2^+$). Additional exothermic products arise from proton transfer ($CD_3NH_3^+$) and from H and D abstraction (NH_4^+, NH_3D^+). Evidence is also given that another product with $m/z=18$ (NH_2D^+) is formed at collision energies above 4.0 eV. A thermoneutral product is also observed with $m/z=32$ that corresponds to $CD_2{=}{=}NH_2^+$. This product likely results from dissociative charge transfer, that is, from a dissociation reaction that occurs on the charge-transfer surface. All three of the high mass ion products ($m/z=32$, 34, 35) are backward scattered in the center-of-mass frame whereas the two low mass ion products ($m/z=18$, 19) are forward scattered, approaching the spectator stripping limit.

The relative cross section for formation of each product is a decreasing function of collision energy at all ammonia vibrational states studied. This behavior is typical for ion–molecule reactions with no threshold energy. Furthermore, the relative values of the reaction cross section for each product, aside from $CD_2{=}{=}NH_2^+$, decreases with increasing energy in the ν_2 mode of the ammonia ion reactant. The cross section for $CD_2{=}{=}NH_2^+$, on the other hand, shows about a two fold enhancement at low collision energies in going from $\nu_2=1$ to $\nu_2=9$, corresponding to a vibrational energy range of 0.12–1.08 eV in the ammonia ion. This trend in cross section vs vibrational energy is opposite to the result observed vs collision energy, which indicates that these two forms of energy are not equivalent in the formation of $CD_2{=}{=}NH_2^+$. Comparison of the branching ratios for the products with $m/z=32$ and 34 obtained from ammonia ions prepared in the nearly isoenergetic $1^0 2^5$ and $1^1 2^2$ states indicates that this reaction is vibrationally mode specific. This mode specificity is consistent with the picture[6] that such behavior is to be expected when the charge-transfer channel is open and competing with other channels in reactions with ammonia ions.

ACKNOWLEDGMENT

The authors gratefully acknowledge the financial support of the Air Force Office of Scientific Research (Grant No. F49620-98-1-0040).

[1] R. A. Dressler and E. Murad, in *Unimolecular and Bimolecular Reaction Dynamics*, edited by C. Y. Ng, T. Baer, and I. Powis (Wiley, Chichester, 1994), p. 87.
[2] J. C. Poutsma, M. A. Everest, J. E. Flad, G. C. Jones, Jr., and R. N. Zare, Chem. Phys. Lett. **305**, 343 (1999).
[3] M. A. Everest, J. C. Poutsma, and R. N. Zare, J. Phys. Chem. A **102**, 9593 (1998).
[4] M. A. Everest, J. C. Poutsma, J. E. Flad, and R. N. Zare, J. Chem. Phys. **111**, 2507 (1999).
[5] L. A. Posey, R. D. Guettler, N. J. Kirchner, and R. N. Zare, J. Chem. Phys. **101**, 3772 (1994).
[6] J. C. Poutsma, M. A. Everest, J. E. Flad, and R. N. Zare, Appl. Phys. B: Lasers Opt. **71**, 623 (2000).
[7] S. L. Anderson, Adv. Chem. Phys. **82**, 177 (1992).
[8] H.-T. Kim, R. J. Green, and S. L. Anderson, J. Chem. Phys. **112**, 10831 (2000).
[9] N. G. Adams, D. Smith, and J. F. Paulson, J. Chem. Phys. **72**, 288 (1980).
[10] *NIST Chemistry WebBook*, edited by W. Mallard (NIST, http://webbook.nist.gov/chemistry, 1998), Vol. 69.
[11] R. D. Guettler, G. C. Jones, Jr., L. A. Posey, N. J. Kirchner, B. A. Keller, and R. N. Zare, J. Chem. Phys. **101**, 3763 (1994).
[12] P. J. Miller, S. D. Colson, and W. A. Chupka, Chem. Phys. Lett. **145**, 183 (1988).
[13] W. E. Conaway, R. J. S. Morrison, and R. N. Zare, Chem. Phys. Lett. **113**, 429 (1985).
[14] D. Gerlich, Adv. Chem. Phys. **82**, 1 (1992).
[15] R. D. Levine and R. B. Bernstein, *Molecular Reaction Dynamics and Chemical Reactivity* (Oxford University Press, New York, 1987).
[16] H.-T. Kim, R. J. Green, and S. L. Anderson, J. Chem. Phys. **113**, 11079 (2000).
[17] D. C. Harris, *Quantitative Chemical Analysis*, 4th ed. (W. H. Freeman and Company, New York, 1995).
[18] A. Sinha, M. C. Hsiao, and F. F. Crim, J. Chem. Phys. **92**, 6333 (1990).

[19] A. Sinha, M. C. Hsiao, and F. F. Crim, J. Chem. Phys. **94**, 4928 (1991).
[20] M. J. Bronikowski, W. R. Simpson, B. Girard, and R. N. Zare, J. Chem. Phys. **95**, 8647 (1991).
[21] M. J. Bronikowski, W. R. Simpson, and R. N. Zare, J. Phys. Chem. **97**, 2194 (1993).
[22] A. Sinha, J. D. Thoemke, and F. F. Crim, J. Chem. Phys. **96**, 372 (1992).
[23] R. D. Guettler, G. C. Jones, Jr., L. A. Posey, and R. N. Zare, Science **266**, 259 (1994).
[24] H. Fu. J. Qian, R. J. Green, and S. L. Anderson, J. Chem. Phys. **108**, 2395 (1998).
[25] G. Mauclair, M. Heninger, S. Fenistein, J. Wronka, and R. Marx, Int. J. Mass Spectrom. Ion Processes **80**, 99 (1987).